Intervalley scattering in GaAs/AlAs resonant-tunneling diodes

Paul Sotirelis and Patrick Roblin
Department of Electrical Engineering, The Ohio State University, Columbus, Ohio 43210
(Received 13 October 1994; revised manuscript received 9 January 1995)

The current-voltage characteristic of a resonant-tunneling diode (RTD) is calculated with and without Γ to X intervalley scattering. The current is determined from the self-consistent solution of the Schrödinger and Poisson equations. We examine a RTD for which the collector, emitter, and central well are GaAs and the barriers are AlAs. Intervalley scattering makes a significant contribution to the current, at voltages above the X-Γ energy offset of the collector.

I. INTRODUCTION

Resonant tunneling diodes[1] (RTD's) are currently of great interest, due to their potential future use in high-speed devices.[2] Applications, such as oscillators,[3] harmonic multipliers,[4] and logic elements[5] are among those recently being investigated. Scattering plays an important role in RTD's by providing additional paths through which an electron can traverse the device via the resonant state. However, including the effects of scattering in quantum mechanical simulations of RTD's is a considerable theoretical challenge.[6] By investigating intervalley scattering in RTD's, we build upon an earlier work,[7] which studied polar-optical phonon, acoustic phonon, interface roughness, and alloy scattering. This is, to our knowledge, the first quantum mechanical simulation of electron transport in RTD's that includes intervalley phonon scattering. In this study, as in Ref. 7, we consider a full three-dimensional treatment of k space.

We simulate electron transport across one-dimensional structures including intervalley phonon scattering. By one-dimensional structures, we mean those that are spatially varying in one direction, and translationally invariant on a similar length scale perpendicular to this direction. The method used is described in Ref. 7, in which the time-dependent Schrödinger equation is solved using an energy expansion and an impulse response technique. Self-consistency is included through an iterative solution with the Poisson equation. A combination Wannier function and plane (Bloch) wave basis provides a convenient discretization along the growth direction (longitudinal) and translational invariance perpendicular to the growth direction (transverse). The time-dependent envelope equation is solved assuming the envelope function to have both an unscattered and scattered part. The scattered part contains an expansion over the phonon wave vector and allows for the inelastic nature of the phonons. The resulting coupled difference equations reduce to a single tight-binding type equation when scattering is turned off. The nonzero coupling term allows for phonon scattering and is described in terms of a self-energy. Reference 7 contains a detailed derivation of this method applied to other scattering mechanisms. We present the coupled difference equations for phonon scattering in Appendix A, for completeness. The details which are unique to intervalley scattering are the derivation of the corresponding self-energy, which is done in Sec. II and the corresponding current, which is done in Sec. III. The numerical results are discussed in Sec. IV and Sec. V presents the conclusion.

The band structure is assumed to be effective mass in the transverse direction and tight binding in the longitudinal direction. That is the electron Hamiltonian in the absence of scattering is given by

$$H^{e}_{nn'}(\mathbf{k}_\perp) = H_{nn'} + \frac{\hbar^2 k_\perp^2}{2m^*_n}\delta_{nn'} ,$$

$$H_{nn'} = -\frac{\hbar^2}{2a^2\sqrt{m^*_n m^*_{n+1}}}\delta_{n+1\,n'} - \frac{\hbar^2}{2a^2\sqrt{m^*_n m^*_{n-1}}}\delta_{n-1\,n'} + \left[\frac{\hbar^2}{a^2 m^*_n} + E^{\mathrm{con}}_n - eV^{\mathrm{app}}_n\right]\delta_{nn'} .$$

The index, n, refers to position, a is the lattice parameter, V^{app} is the applied electrostatic potential, and $\mathbf{k}_\perp$ is the wave vector in the transverse direction. The spatially varying effective mass, m^*, and the conduction band edge, E^{con}, are set to either Γ-valley or X-valley values, depending which valley the electron occupies. The elliptical energy surfaces associated with the X-valley are treated as spherical, using the density of states effective mass for GaAs and AlAs.[8] We assume that the only electrons that transfer to the X valley are those that have undergone Γ to X intervalley phonon scattering. The transfer due to band mixing which has been previously studied in single layer heterostructures,[9] in RTD's,[10] and in superlattices,[11] is entirely neglected. This has been shown to be a good approximation for the barrier thickness under consideration in this paper.[12]

In contrast to the spatially varying band structure, the deformation potentials and phonon frequencies are approximated by their bulk values. The justification being that these crystal properties appear in only the weaker scattering part of the solution. An additional justification involves sacrificing some accuracy for a quicker and more robust solution. We use the bulk deformation po-

tentials given in Ref. 13. From symmetry considerations, the only phonons that contribute to Γ to X transitions are LOX phonons;[14] the phonon frequencies that we use are also from Ref. 13.

II. SELF-ENERGY

Our method requires that we calculate the matrix element of the electron-phonon Hamiltonian in the combined Wannier-plane-wave basis. In Ref. 7, we considered the electron-phonon Hamiltonian given by

$$H_{\text{el-ph}}(\mathbf{r},t)=\frac{i}{\sqrt{V}}\sum_{\mathbf{q}}\alpha_{\mathbf{q}}[a_{\mathbf{q}}e^{i\mathbf{q}\cdot\mathbf{r}}-a_{\mathbf{q}}^{\dagger}e^{-i\mathbf{q}\cdot\mathbf{r}}]\,, \tag{1}$$

where V is the volume of the crystal, $\mathbf{q}$ is the phonon mode, $a_{\mathbf{q}}$ and $a_{\mathbf{q}}^{\dagger}$ are the creation and annihilation operators, and $\alpha_{\mathbf{q}}$ gives the coupling strength, unique to the particular phonon scattering mechanism. For intervalley scattering, we compare the matrix element of Eq. (1) with Eq. (14) of Ref. 15, and make the following correspondence $\alpha_{\mathbf{q}}^2=\hbar D_{\mathbf{q}}^2/(2\rho\omega_{\mathbf{q}})$. The deformation potential, $D_{\mathbf{q}}$, is assumed to be independent of the electrons initial wave vector. We assume a translationally invariant deformation potential given by an average of those for GaAs and AlAs. The density of the crystal, ρ, and phonon frequency, $\omega_{\mathbf{q}}$, are also assumed to be translationally invariant and given by their GaAs values.

Detailed in Ref. 7 and summarized in Appendix A is the description of how phonon scattering is included in the transport equations. A given scattering mechanism is included through an additional term, $G(n)$, relating to its self-energy. The expression, $G(n)=\sum_m H_{\text{SE}}(n,m)f_0(m)$, describes the connection between $G(n)$, the self-energy (H_{SE}), and the unscattered part of the envelope function (f_0). We proceed to calculate the self-energy by determining the function $G(n)$. The function, $G(n)$, for intervalley phonon scattering is, with the above $\alpha_{\mathbf{q}}$, given by

$$\begin{aligned}G(n)&=G^{+}(n)+G^{-}(n)\\&=\frac{1}{L_x}\sum_{q_x>0}\sin(q_xna)\frac{1}{S}\sum_{\mathbf{q}_\perp}N_{\mathbf{q}}(2\alpha_{\mathbf{q}})^2f_1(n,q_\perp,q_x)+\frac{1}{L_x}\sum_{q_x>0}\sin(q_xna)\frac{1}{S}\sum_{\mathbf{q}_\perp}(N_{\mathbf{q}}+1)(2\alpha_{\mathbf{q}})^2f_1(n,q_\perp,q_x).\end{aligned} \tag{2}$$

The plus term represents absorption and the minus represents emission. The factors L_x and S are the normalization length and area, respectively. $N_{\mathbf{q}}$ is the Bose statistical factor and $f_1(n,q_\perp,q_x)$ is the part of the envelope function associated with the scattered wave. We assume that $\omega_{\mathbf{q}}=\omega_{ij}$, $N(\omega_{\mathbf{q}})=N(\omega_{ij})$, and $\alpha_{\mathbf{q}}=\alpha_{ij}$ throughout the entire derivation,[16] where ω_{ij} is the LOX-phonon frequency. Rewriting Eq. (2), we obtain the following:

$$\begin{aligned}G(n)=&\frac{1}{L_x}\sum_{q_x>0}\sin(q_xna)\,N_{ij}(2\alpha_{ij})^2\\&\times\frac{1}{S}\sum_{\mathbf{q}_\perp}f_1(n,q_\perp,q_x)\\&+\frac{1}{L_x}\sum_{q_x>0}\sin(q_xna)\,(N_{ij}+1)(2\alpha_{ij})^2\\&\times\frac{1}{S}\sum_{\mathbf{q}_\perp}f_1(n,q_\perp,q_x).\end{aligned} \tag{3}$$

For convenience, the summation over $\mathbf{q}_\perp$ is transformed into an integration over E_{1x}, which is defined below. For consistency with Ref. 7, some variables associated with the initial valley i (final valley j) have subscripts, denoted as 0 (1). Even though a spatially varying band structure is being used, a fixed lattice point is used as a reference for the energy. Therefore, the energies E_{1x}, E_{0x}, Δ_1, Δ_0, and the masses m_1 and m_0, all are with reference to the first lattice site. Conservation of energy is expressed below for an electron scattering from the Γ to the X valley:

$$\begin{aligned}&E_{1x}+\Delta_1+\frac{\hbar^2}{2m_1^*}|\mathbf{k}_{0\perp}-\mathbf{X}_\perp\pm\mathbf{q}_\perp|^2\\&\quad=E_{0x}+\Delta_0+\frac{\hbar^2k_{0\perp}^2}{2m_0^*}\pm\hbar\omega_{ij}.\end{aligned} \tag{4}$$

The vector, $\mathbf{X}_\perp$, allows for the displacement in k space of X with respect to Γ and is given by $\mathbf{X}_\perp=(0,0,2\pi/a)$ (Ref. 17), where a is the lattice parameter. We choose θ to be the angle between $\mathbf{k}_{0\perp}-\mathbf{X}_\perp$ and $\mathbf{q}_\perp$, and introduce the wave vector $\mathbf{K}_{0\perp}$, which is defined by $\mathbf{K}_{0\perp}=\mathbf{k}_{0\perp}-\mathbf{X}_\perp$. Equation (4) is rewritten below:

$$\begin{aligned}&\frac{\hbar^2}{2m_1^*}\left(K_{0\perp}^2\left[1-\frac{m_1^*k_{0\perp}^2}{m_0^*K_{0\perp}^2}\right]\pm2K_{0\perp}q_\perp\cos\theta+q_\perp^2\right)\\&\quad+\Delta_1-\Delta_0+E_{1x}-E_{0x}\mp\hbar\omega_{ij}=0.\end{aligned} \tag{5}$$

Equation (5) contains two equations, one for absorption and one for emission corresponding to the plus and minus signs. For convenience, Eq. (5) is abbreviated by the expression, $E_{1x}-E^{\pm}(q_\perp,\theta)=0$. The transformation, $q_\perp\rightarrow E_{1x}$, proceeds as follows:

$$\begin{aligned}&\sum_{\mathbf{q}_\perp}f_1(n,q_\perp,q_x)\\&\quad=\int dE_{1x}\sum_{\mathbf{q}_\perp}f_1(n,q_\perp(E_{1x}),q_x)\,\delta\left[E_{1x}-E^{\pm}(q_\perp,\theta)\right]\\&\quad=\int dE_{1x}\,f_1(n,E_{1x},q_x)\sum_{\mathbf{q}_\perp}\delta\left[E_{1x}-E^{\pm}(q_\perp,\theta)\right].\end{aligned}$$

The summation over $\mathbf{q}_\perp$ using the δ function is done as follows:

$$I = \sum_{\mathbf{q}_\perp} \delta\left[E_{1x} - E^+(q_\perp,\theta)\right] + \sum_{\mathbf{q}_\perp} \delta\left[E_{1x} - E^-(q_\perp,\theta)\right]$$

$$= \frac{S}{(2\pi)^2}\frac{2m_1^*}{\hbar^2}\int_0^{2\pi} d\theta \int_0^{\infty} dq_\perp\, q_\perp \sum_{i=1}^{2} \frac{\delta[q_\perp - q_{0,i}^+(\theta)]}{2|q_{0,i}^+(\theta) + K_{0\perp}\cos\theta|}$$
$$+ \frac{S}{(2\pi)^2}\frac{2m_1^*}{\hbar^2}\int_0^{2\pi} d\theta \int_0^{\infty} dq_\perp\, q_\perp \sum_{i=1}^{2} \frac{\delta[q_\perp - q_{0,i}^-(\theta)]}{2|q_{0,i}^-(\theta) - K_{0\perp}\cos\theta|}.$$

The zeros of the δ function for absorption and emission are denoted by $q_{0,i}^+(\theta)$ and $q_{0,i}^-(\theta)$, respectively. Each zero is a solution of a quadratic equation and, therefore, has two possible solutions which correspond to $i = 1, 2$. We choose the $i = 1$ root to be denoted as $q_{0,+}^{\pm}(\theta)$ and the $i = 2$ root to be denoted as $q_{0,-}^{\pm}(\theta)$. Their values are given explicitly in Appendix B. Upon integrating over $q_\perp$ with the use of the δ functions, we arrive at the following:[18]

$$I = \frac{S}{(2\pi)^2}\frac{m_1^*}{\hbar^2}\int_0^{2\pi} d\theta\ (\Theta[q_{0,+}^+(\theta)] + \Theta[q_{0,-}^+(\theta)] + \Theta[q_{0,+}^-(\theta)] + \Theta[q_{0,-}^-(\theta)]).$$

The step functions as a function of θ are nonzero only if the δ functions contribute upon the $q_\perp$ integration. The conditions for q_0^+ and q_0^- to be in the range of $q_\perp$ integration are $q_0^{\pm}(\theta) > 0$. Appendx B contains the details of the evaluation of the angular integral. The result is given below:

$$I = \frac{S}{(2\pi)^2}\frac{2\pi\, m_1^*}{\hbar^2}\left[g(A[E_{1x}]) + g(B[E_{1x}])\right],$$

$$A[E_{1x}] = 1 - \frac{m_1^* k_{0\perp}^2}{m_0^* K_{0\perp}^2} + \frac{2m_1^*}{\hbar^2 K_{0\perp}^2}\left[E_{1x} - E_{0x} + \Delta_1 - \Delta_0 - \hbar\omega_{ij}\right],$$

$$B[E_{1x}] = 1 - \frac{m_1^* k_{0\perp}^2}{m_0^* K_{0\perp}^2} + \frac{2m_1^*}{\hbar^2 K_{0\perp}^2}\left[E_{1x} - E_{0x} + \Delta_1 - \Delta_0 + \hbar\omega_{ij}\right].$$

The function $g(A:B)$ ranges in value from zero to one. Using the result for the integral, I, the function, $G(n)$ is expressed as an integration over E_{1x} instead of a summation over $\mathbf{q}_\perp$. Therefore, Eq. (3) is rewritten below:

$$G(n) = \frac{1}{L_x}\sum_{q_x>0}\sin(q_x n a)N_{ij}(2\alpha_{ij})^2 \times\frac{1}{(2\pi)^2}\frac{2\pi m_1^*}{\hbar^2}\int dE_{1x} f_1(n, E_{1x}, q_x)g(A[E_{1x}]) + \frac{1}{L_x}\sum_{q_x>0}\sin(q_x n a)(N_{ij}+1)(2\alpha_{ij})^2 \times\frac{1}{(2\pi)^2}\frac{2\pi m_1^*}{\hbar^2}\int dE_{1x} f_1(n, E_{1x}, q_x)g(B[E_{1x}]). \quad (6)$$

The final step, necessary in order to express the self-energy in its desired form, is to write $G(n)$ in terms of $f_0(n)$. We use the impulse response technique outlined in Appendix A. The impulse response function, $h_{nm}(E_{1x})$, is defined by the following equation,

$$E_{1x}h_{nm}(E_{1x}) = \sum_l \tilde{H}_{nl}\, h_{lm}(E_{1x}) + \delta_{nm}.$$

With this definition the transport equation [Eq. (A2)] is automatically satisfied if $f_1(n, E_{1x}, q_x)$ is written in the following form:

$$f_1(n, E_{1x}, q_x) = \sum_m h_{nm}(E_{1x})\sin(q_x m a) f_0(m).$$

We also make use of the following sum over the longitudinal phonon modes, q_x:

$$\sum_{q_x>0}\sin(q_x n a)\sin(q_x m a) = \frac{L_x q_{x,\max}}{4\pi}\delta_{nm}. \quad (7)$$

The maximum value of the longitudinal phonon wave vector, $q_{x,\max}$, is given by its bulk value $2\pi/a$. The resulting equation for $G(n)$ is written below:

$$G(n) = \frac{1}{2a}N_{ij}(2\alpha_{ij})^2 f_0(n) \times\frac{1}{(2\pi)^2}\frac{2\pi m_1^*}{\hbar^2}\int dE_{1x} h_{nn}(E_{1x})g(A[E_{1x}]) + \frac{1}{2a}(N_{ij}+1)(2\alpha_{ij})^2 f_0(n) \times\frac{1}{(2\pi)^2}\frac{2\pi m_1^*}{\hbar^2}\int dE_{1x} h_{nn}(E_{1x})g(B[E_{1x}]). \quad (8)$$

In the above form, the difference equations are decoupled as described in Appendix A and an $N \times N$ linear system remains to be solved for $f_0(n)$, where N is the total number of lattice sites.

III. CURRENT SUMMATION

In this section, we derive the portion of the transmitted current associated with the scattered electrons in the X valley. The calculation of the net current across the device is outlined in Appendix C. The transmitted current for phonon scattering is written below as (a similar equation gives the reflected current)

$$J_T^{\text{scat}\,\pm}(E_{0x}, E_{0\perp}) = \frac{e}{L_x} \sum_{q_x>0} \frac{1}{S} \sum_{\mathbf{q}_\perp} \left(N_{\mathbf{q}} \mp \frac{1}{2} + \frac{1}{2} \right) \times (2\alpha_{\mathbf{q}})^2 |f_1(N, E_{1x}, q_x)|^2 v_R(E_{1x}). \tag{9}$$

Notice the envelope function, $f_1(N, E_{1x}, q_x)$, is evaluated at the last lattice site ($n = N$). Also note that the electron's group velocity at the right contact is denoted as $v_R(E_{1x})$. See Appendix C for the definition of the electron velocity, which is determined by the band structure. The above expression is evaluated in a similar manner as was the self-energy. The summation over $\mathbf{q}_\perp$ is transformed into an integration over E_{1x}. The summation over q_x is performed using Eq. (7); notice that the cross terms are zero upon the q_x integration, as is illustrated below:

$$\begin{aligned} \sum_{q_x} & |f_1(N, E_{1x}, q_x)|^2 \\ &= \sum_{q_x} \left(\sum_m h_{Nm}(E_{1x}) \sin(q_x m a) f_0(m) \right)^* \\ &\quad \times \left(\sum_n h_{Nn}(E_{1x}) \sin(q_x n a) f_0(n) \right) \\ &= \frac{L_x q_{x,\max}}{4\pi} \sum_m |h_{Nm}(E_{1x})|^2 |f_0(m)|^2. \end{aligned}$$

The resulting expression for $J_T(E_{0x}, E_{0\perp})$ is given by

$$\begin{aligned} J_T^{\text{scat}}(E_{0x}, E_{0\perp}) = {} & e \frac{1}{2a} N_{ij} (2\alpha_{ij})^2 \frac{1}{(2\pi)^2} \frac{2\pi m_1^*}{\hbar^2} \int dE_{1x} g(A[E_{1x}]) \sum_n |h_{Nn}(E_{1x})|^2 |f_0(n)|^2 v_R(E_{1x}) \\ & + e \frac{1}{2a} (N_{ij} + 1)(2\alpha_{ij})^2 \frac{1}{(2\pi)^2} \frac{2\pi m_1^*}{\hbar^2} \int dE_{1x} g(B[E_{1x}]) \sum_n |h_{Nn}(E_{1x})|^2 |f_0(n)|^2 v_R(E_{1x}). \end{aligned} \tag{10}$$

This current is used to calculate the transmission probability, which in turn is used to determine the net current across the device, as explained in Ref. 7. So the effect of scattering on the current is entirely included in the modified transmission probability. All electrons are assumed to be in the Γ valley unless scattered into the X valley. We consider at most one scattering event per electron. Therefore, the scattered electrons within the X valley continue unscattered. Thermal equilibrium is assumed in the right and left contacts.

It is interesting to note that the self-energy matrix, $H_{\text{SE}}(n, m)$, is diagonal which is typical of a local scattering process. However, phonon scattering is a nonlocal scattering process. This reduction to a local process results from the summation over the longitudinal wave vector, q_x, which was done analytically. This analytic summation is possible because of the approximation that $\alpha_{\mathbf{q}}$ is independent of $\mathbf{q}$. The final form of the current, $J_T(E_{0x}, E_{0\perp})$, is also characteristic of a local scattering process. As shown above, the current's form goes from nonlocal to local when the magnitude squared of the sum of terms ($|\sum h(m) f_0(m) \sin(q_x m a)|^2$) is simplified to the sum of the magnitude squared terms ($\sum |h(m)|^2 |f_0(m)|^2$).

IV. NUMERICAL RESULTS

We consider a test structure with two GaAs spacers (emitter and collector), a GaAs quantum well, and AlAs barriers. The test structure has barrierwidths of four monolayers and is symmetric. We use a relatively wide quantum well of 14 monolayers, in order to have a low resonance energy. The spacers, the undoped regions between the barriers and the doped regions, have widths of seven monolayers. The discretization scheme consists of 36 equally spaced sites with an intersite distance corresponding to a single monolayer. We refer to the region composed of the spacers, barriers, and quantum well as the quantum region, since it is in this region for which the Schrödinger equation is solved. This yields a quantum region of approximately 100 Å. Outside the quantum region, are the doped contacts which we refer to as the contacts or leads.

Our choice of device size and barrier widths were influenced by computational issues, which are important when including scattering. The memory requirements scale as the square of the device size, whether or not scattering is included. We expect the effect of intervalley scattering to increase with the barrier thickness. Unfortunately, increasing the barrier width decreases the transmission resonance width, which compounded with scattering can make it difficult to achieve a desirable current error. Therefore, we chose relatively thin barriers and spacers. The test structure assumes doping levels of $5 \times 10^{18}\,\text{cm}^{-3}$ at each contact, and self-consistency is enforced through use of the Poisson equation. The current scales linearly with the device area, which is $1\,\text{m}^2$. The X-Γ offset energy is 0.48 eV for GaAs and -0.92 eV for AlAs. The GaAs Γ-valley to AlAs Γ-valley discontinuity is 1.11 eV. The GaAs Γ-valley to AlAs X-valley discontinuity is 0.19 eV. The temperature is 300 K. Figure 1 plots the Γ and X valleys, versus position for a subset of the voltages dropped across the quantum region. Note, the leftmost Γ potential is the reference energy as described earlier, but is not set to zero because of our contact model.

For electrons traveling to the right, their scattering to the X valley only contributes to the current if their lon-

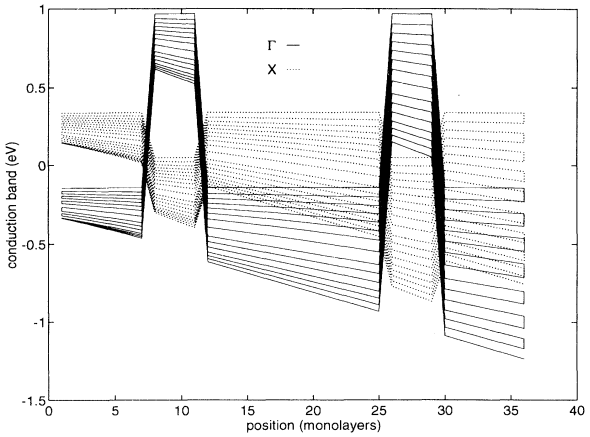

FIG. 1. The conduction band is plotted versus position for a range of voltages across the quantum region. The Γ valley is given by the solid line and the X valley is given by the dotted line.

gitudinal energy is greater than the X-valley minimum at the right most contact. This is assured for electrons at each energy when the bias across the quantum region is greater than the X-Γ offset energy of GaAs.[19] Therefore, we expect intervalley scattering to be most significant for biases above the Γ-X energy offset (for GaAs). In Fig. 2, the current with and without intervalley scattering, is plotted versus the voltage dropped across the quantum region. At high voltages, it is shown that intervalley scattering makes a significant contribution to the current. The minimum voltage for which intervalley scattering contributes to the current matches extremely well with the X-Γ energy offset of 0.48 eV.

In addition, we see that intervalley scattering has an effect, even at lower voltages. There is a noticeable change in the current-voltage characteristic below the X-Γ offset energy. The current peak is almost rigidly shifted to a slightly lower voltage if intervalley scattering is included. In Fig. 3, the transmission probability is plotted versus energy with and without scattering for a voltage across the quantum region of 0.1 Volts. The transmission peak is shifted, but not significantly broadened. This indicates a shift of the resonant energy level, but without much additional broadening. This is characteristic of a discrete energy state coupled to a continuum of states whose energy range excludes the discrete state.[20] The implication is that, at low voltages, intervalley scattering introduces additional coupling, to states with energies different from the resonant ground state. This should not be too surprising since, at low voltages, the X-valley continuum (spacers and well) is above the resonant ground state. In our model, we actually have a slightly broadened and shifted state in the above situation, instead of a discrete state because of the finite barrier widths.

The increase in the current at higher voltages is attributed to the same quantum mechanical effect. Only it is due to the first excited state being shifted; the ground state is energetically inaccessible at these higher voltages. In Fig. 4, the transmission probability is plotted versus energy with and without scattering for a voltage across the quantum region of 0.7 Volts. The energy shift is much larger than for the ground state, and is accompanied by broadening as well. We would like to point out that it is the energy shift that is particularly important in regard to the effect of intervalley scattering on the current. This is because the injected electrons obey a thermal distribution and, therefore, sample only the low energy part of this peak. We emphasize that well over (95%) of the current remains in the Γ valley, even at high voltages,

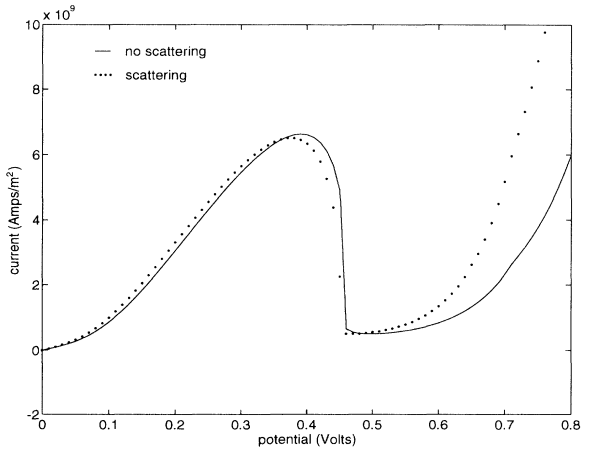

FIG. 2. The current is plotted versus the voltage across the quantum region. The voltage across the leads is excluded. The solid curve gives the current without scattering and the dotted curve gives the current with intervalley scattering included.

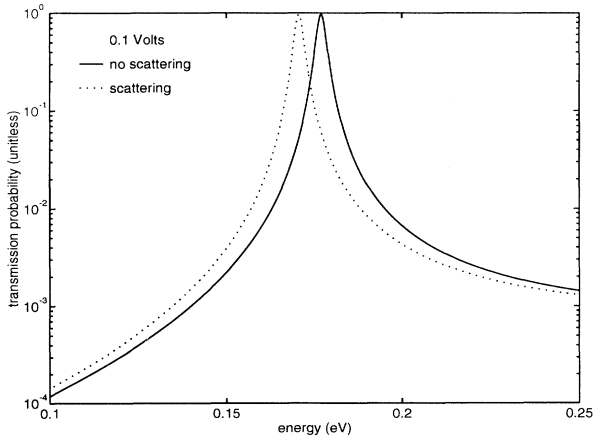

FIG. 3. The transmission probability is plotted versus the longitudinal energy. The solid curve gives the probability without scattering and the dotted curve gives the probability with intervalley scattering included. The voltage across the quantum region is 0.1 V.

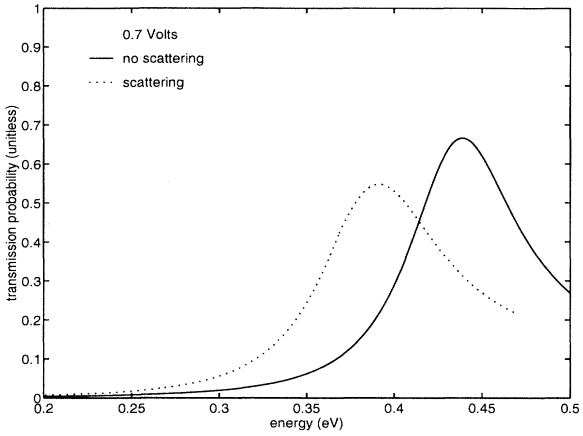

FIG. 4. The transmission probability is plotted versus the longitudinal energy. The solid curve gives the probability without scattering and the dotted curve gives the probability with intervalley scattering included. The voltage across the quantum region is 0.7 V.

and that it is the shift of the resonant energy that is responsible for the increased current.

We also point out the lack of any secondary peaks in the transmission probability, which are present for polar-optical phonon scattering. This implies that intervalley scattering primarily occurs from the resonant state to the collector, rather than into the resonant state from the emitter. This is expected, since a right traveling electron has significantly more kinetic energy available on the collector side.

V. CONCLUSION

The current-voltage characteristic of an RTD is determined by solving the time-dependent Schrödinger equation with and without intervalley scattering. We conclude that intervalley scattering makes a significant contribution to the current, at voltages above the X-Γ energy offset of the collector. The significant increase in the current, at high voltages, is shown to be due to a scattering-induced downward shift in the energy of the first excited resonant state. We also explain the rigid shift of the current peak to lower voltages, as due to the scattering-induced downward shift in energy of the resonant ground state.

ACKNOWLEDGMENTS

We would like to thank Dejan Jovanovic and Roger Lake for useful discussions and acknowledge support from Texas Instruments.

APPENDIX A: THE DIFFERENCE EQUATIONS

We present the coupled difference equations that describe transport across one-dimensional structures in the presence of phonon scattering. The notation is similar to that in Ref. 7, except $G(n)$, defined by Eq. (2), implicitly includes the q_x summation. $\tilde{H}_{nm}$ represents the heterostructure Hamiltonian, including the applied voltage, effective mass in the transverse direction and tight binding in the longitudinal direction [see Eq. (6) of Ref. 7]. The coupled difference equations are given below:

$$E_{0x} f_0(n) = \sum_m \tilde{H}_{nm}\, f_0(m) + G(n) \tag{A1}$$

$$E_{1x} f_1(n, E_{1x}, q_x) = \sum_m \tilde{H}_{nm}\, f_1(m, E_{1x}, q_x) + \sin(q_x n a)\, f_0(n). \tag{A2}$$

The energies E_{0x} and E_{1x}, and the function $G(n)$ are defined in Sec. II for intervalley scattering. The above difference equations are decoupled by using the impulse response function (the sine factor is missing in Ref. 7), as follows:

$$f_1(n, E_{1x}, q_x) = \sum_m h_{nm}(E_{1x}) \sin(q_x m a) f_0(m). \tag{A3}$$

Equation (A3) is substituted into the expression for $G(n)$ given by Eq. (6). Therefore, $G(n)$ has a dependence on $f_0(n)$ instead of $f_1(n, E_{1x}, q_x)$. This allows for a decoupling of Eqs. (A1) and (A2) along with defining the self-energy, $H_{\mathrm{SE}}(n,m)$, as $G(n) = \sum_m H_{\mathrm{SE}}(n,m) f_0(m)$. The self-energy is used to solve for the envelope function, $f_0(n)$ and later to solve for the current, $J_T(E_{0x}, E_{0\perp})$. The impulse response function is defined below:

$$E_{1x} h_{nm}(E_{1x}) = \sum_l \tilde{H}_{nl}\, h_{lm}(E_{1x}) + \delta_{nm}. \tag{A4}$$

APPENDIX B: THE θ INTEGRATION

We solve the following angular integral:

$$I = \frac{S}{(2\pi)^2} \frac{m_1^*}{\hbar^2} \int_0^{2\pi} d\theta \left(\Theta[q_{0,+}^+(\theta)] + \Theta[q_{0,-}^+(\theta)] + \Theta[q_{0,+}^-(\theta)] + \Theta[q_{0,-}^-(\theta)]\right),$$

with the zeros given by

$$q_{0,\pm}^+(\theta) = -K_{0\perp} \cos\theta \pm \sqrt{K_{0\perp}^2 \cos^2\theta - K_{0\perp}^2 \left[1 - \frac{m_1^* k_{0\perp}^2}{m_0^* K_{0\perp}^2}\right] - \frac{2m_1^*}{\hbar^2} [E_{1x} - E_{0x} + \Delta_1 - \Delta_0 - \hbar\omega_{ij}]},$$

$$\cos^2\theta > 1 - \frac{m_1^* k_{0\perp}^2}{m_0^* K_{0\perp}^2} + \frac{2m_1^*}{\hbar^2 K_{0\perp}^2} [E_{1x} - E_{0x} + \Delta_1 - \Delta_0 - \hbar\omega_{ij}]$$

and

$$q_{0,\pm}^{-}(\theta) = +K_{0\perp}\cos\theta \pm \sqrt{K_{0\perp}^2\cos^2\theta - K_{0\perp}^2\left[1-\frac{m_1^* k_{0\perp}^2}{m_0^* K_{0\perp}^2}\right] - \frac{2m_1^*}{\hbar^2}\left[E_{1x}-E_{0x}+\Delta_1-\Delta_0+\hbar\omega_{ij}\right]},$$

$$\cos^2\theta > 1 - \frac{m_1^* k_{0\perp}^2}{m_0^* K_{0\perp}^2} + \frac{2m_1^*}{\hbar^2 K_{0\perp}^2}\left[E_{1x}-E_{0x}+\Delta_1-\Delta_0+\hbar\omega_{ij}\right].$$

The step functions are nonzero when $q_0^+(\theta)$ and $q_0^-(\theta)$ are real and positive, and, therefore, in the range of the previous integration over $q_\perp$. Using the above conditions, the step functions are simplified as follows:

$$\Theta[q_{0,+}^+(\theta)] + \Theta[q_{0,-}^+(\theta)]$$

$$= \Theta(\cos^2\theta - A)\Theta(-A) + \Theta(\cos^2\theta - A)\Theta(A)$$
$$= \Theta(\cos^2\theta - A)$$

and

$$\Theta[q_{0,+}^-(\theta)] + \Theta[q_{0,-}^-(\theta)]$$

$$= \Theta(\cos^2\theta - B)\Theta(-B) + \Theta(\cos^2\theta - B)\Theta(B)$$
$$= \Theta(\cos^2\theta - B).$$

The constants, $A[E_{1x}]$ and $B[E_{1x}]$, are given in Sec. II. The angular integral is rewritten and completed below:

$$I = \frac{S}{(2\pi)^2}\frac{m_1^*}{\hbar^2}\int_0^{2\pi} d\theta\left[\Theta(\cos^2\theta - A) + \Theta(\cos^2\theta - B)\right]$$
$$= \frac{S}{(2\pi)^2}\frac{m_1^*}{\hbar^2}\,2\pi\,[g(A)+g(B)].$$

The function $g(X)$, which ranges between zero and one is defined below (X assumes the value of A or B, above):

$$2\pi g(X) = 2\left\{\begin{array}{cc} \pi & X<0 \\ 2\cos^{-1}(\sqrt{X}) & 0<X<1 \\ 0 & X>1 \end{array}\right\}.$$

APPENDIX C: CURRENT

The method used to calculate the net current is described in Ref. 7 and is summarized here for completeness. The method is based on a generalization of the Tsu-Esaki formula,[21] involving the transmission coefficient's dependence on energy. We allow the transmission coefficient to depend on the energy associated with the transverse direction ($E_{0\perp}$), as well as the energy associated in the longitudinal direction (E_{0x}). The net current is the difference between the left going current and right going current.

As a first step, we calculate the transmission coefficient for an electron traversing the resonant tunneling diode from left to right. We assume the envelope function, $f_0(n)$, has a flat band form, at the boundaries of the quantum region. Therefore, we consider an additional lattice site on each side of the quantum region. Accordingly, on the left side (emitter), we have

$$f_0(n) = \exp(ik_{0x}^l na) + b_0\exp(-ik_{0x}^l na).$$

On the right side (collector), we have

$$f_0(n) = c_0\exp(ik_{0x}^r na).$$

The wave vectors k_{0x}^l and k_{0x}^r are obtained for a given energy E_{0x} from the tight-binding band structure of the left and right contact, given by

$$E_{0x} = A_l - A_l\cos k_{0x}^l$$
$$= A_r - A_r\cos k_{0x}^r.$$

The numerical solution for $f_0(n)$ inside the quantum region is matched to the above form at the right and left contact. As a result, the incident and transmitted currents for the envelope function, f_0, are determined to be

$$J_I(E_{0x}) = ev_l(E_{0x})$$
$$J_T(E_{0x}) = e|f_0(N)|^2 v_r(E_{0x}).$$

The rightmost lattice site in the quantum region is labeled by N, $v_l(E_{0x})$ is the electron velocity at the left boundary, and $v_r(E_{0x})$ is the electron velocity at the right boundary. The left and right velocities are determined from the tight-binding band structure, given by

$$v_i(E_{0x}) = \frac{1}{\hbar}\frac{dE_{0x}}{dk_{0x}^i},$$

where i is r or l. The transmitted current associated with the envelope function $f_1(n,\mathbf{q})$ is given by

$$J_T^{\rm scat}(E_{0x}, E_{0\perp}, \mathbf{q})$$

$$= e(N_{\mathbf{q}}+1)\frac{(2\alpha_{\mathbf{q}})^2}{V}|f_1(N,\mathbf{q})|^2 v_R(E_{1x})$$
$$+eN_{\mathbf{q}}\frac{(2\alpha_{\mathbf{q}})^2}{V}|f_1(N,\mathbf{q})|^2 v_R(E_{1x}),$$

where the emission and absorption terms are written separately. Notice the scattered current depends on the particular phonon mode, having wave vector $\mathbf{q}$. The transmitted current resulting from considering all the phonon modes is given by

$$J_T^{\rm scat}(E_{0x}, E_{0\perp}) = \sum_{\mathbf{q}} J_T^{\rm scat}(E_{0x}, E_{0\perp}, \mathbf{q}). \qquad \text{(C1)}$$

In Sec. III, Eq. (C1) is used as the starting point in the derivation of the current, due to intervalley phonon scattering. The total transmission coefficient for electrons traversing from left to right, $T_{l\to r}$ is given by

$$T_{l\to r}(E_{0x}, E_{0\perp}) = \frac{J_T(E_{0x}) + J_T^{\text{scat}}(E_{0x}, E_{0\perp})}{J_I(E_{0x})}.$$

In order to calculate the total current across the device it is necessary to consider incident electrons impinging from the right contact as well. The total transmission coefficient for electrons traversing from right to left, $T_{r\to l}(E_{0x}, E_{0\perp})$ is determined by considering the reverse structure and voltage. The net current is the difference between the left and the right going current and is given by

$$\begin{aligned} I_{\text{net}} &= I_{l\to r} - I_{r\to l} \\ &= \frac{m_l^* e}{2\pi^2\hbar^3}\int dE_{0x}\int dE_{0\perp}\frac{T_{l\to r}(E_{0x}, E_{0\perp})}{1+\exp[(E_{0x}+E_{0\perp}-\mu^l)/kT]} \\ &\quad - \frac{m_r^* e}{2\pi^2\hbar^3}\int dE_{0x}\int dE_{0\perp}\frac{T_{r\to l}(E_{0x}, E_{0\perp})}{1+\exp[(E_{0x}+E_{0\perp}-\mu^r)/kT]}, \end{aligned}$$

where $m_{r,l}^*$ are the electrons Γ-valley effective masses at the right and left contacts, e is the charge of an electron, and $\mu^{r,l}$ are the chemical potentials at the right and left contacts.

[1] L. L. Chang, L. Esaki, and R. Tsu, Appl. Phys. Lett. **24**, 593 (1974).

[2] H. C. Liu and T. C. L. G. Sollner, in *Semiconductors and Semimetals*, edited by R. K. Willardson, A. C. Beer, and E. R. Weber (Academic, New York, 1994), Vol. 41.

[3] E. R. Brown, J. R. Söderström, C. D. Parker, L. J. Mahoney, K. M. Molvar, and T. C. McGill, Appl. Phys. Lett. **58**, 2291 (1991).

[4] A. Rydberg and H. Grönqvist, Electron. Lett. **25**, 348 (1989).

[5] A. C. Seabaugh, Y. C. Kao, and H. T. Yuan, IEEE Electron Device Lett. **13**, 479 (1992).

[6] A lengthy list of references plus an excellent overview concerning scattering in RTD's can be found in R. Lake and S. Datta, Phys. Rev. B **45**, 6670 (1992). Other works include F. Chevior and B. Vinter, Surf. Sci. **229**, 158 (1990); W. R. Frensley, Rev. Mod. Phys. **62**, 745 (1990); U. Ravaioli, M. A. Osman, W. Potz, N. Kluksdahl, and D. K. Ferry, Physica **134B**, 36 (1985).

[7] P. Roblin and W. Liou, Phys. Rev. B **47**, 2146 (1993).

[8] S. Adachi, *Properties of Aluminum Gallium Arsenide* (INSPEC, London, 1993).

[9] H. C. Liu, Appl. Phys. Lett. **51**, 1019 (1987).

[10] P. Roblin, Superlatt. Microstruct. **43**, 363 (1988).

[11] O. E. Raichev, Phys. Rev. B **49**, 5448 (1994); this paper also investigates intervalley phonon scattering in superlattices.

[12] A. R. Bonnefoi, T. C. McGill, R. D. Burnham, and G. B. Anderson, Appl. Phys. Lett. **50**, 344 (1987).

[13] J. Q. Wang, Z. Q. Gu, M. F. Li, and W. Y. Lai, Phys. Rev. B **46**, 12 358 (1992).

[14] S. Zollner, S. Gopalan, and M. Cardona, Appl. Phys. Lett. **54**, 614 (1989).

[15] S. Zollner, S. Gopalan, and M. Cardona, J. Appl. Phys. **68**, 1682 (1990).

[16] E. M. Conwell, in *Solid State Physics: Advances in Research and Applications*, edited by F. Seitz, D. Turnbull, and H. Ehrenreich (Academic, New York, 1967), Suppl. 9.

[17] Choosing between the y or z direction is equivalent, only the magnitude is used.

[18] For each step function there is an additional term which is dropped. This term is determined by rewriting terms of the following form $q_0(\theta)/|q_0(\theta)+K_{0\perp}\cos\theta|$ as $1\pm f(\cos\theta)$. The additional terms yield zero upon the θ integration.

[19] The quasi-Fermi levels are taken into account to get the total voltage across the device.

[20] C. Cohen-Tannoudji, B. Diu, and F. Laloë, *Quantum Mechanics* (Wiley, New York, 1977), Vol. 2, p. 1343.

[21] R. Tsu and L. Esaki, Appl. Phys. Lett. **22**, 562 (1973).